

# INSAR RAILWAY MONITORING VALIDATION THROUGH HIGH DENSITY LEVELING CAMPAIGN

*Qingli Luo<sup>1,2\*</sup>, Guoqing Zhou<sup>2</sup>, Daniele Perissin<sup>3</sup>*

<sup>1</sup> Center of Remote Sensing, Tianjin University, No. 92, Weijin Road, Nankai District, Tianjin 300072, China

<sup>2</sup> Guangxi Key Laboratory for Spatial Information and Geomatics, Guilin University of Technology, Guilin 541004, PR China

<sup>3</sup> School of Civil Engineering, Purdue University, 550 Stadium Mall Drive, West Lafayette, IN 47907–2051, USA

\* Corresponding author, E-Mail: luoqingli2003@163.com

## ABSTRACT

Much attention was paid on monitoring of the subsidence along large-scale man-made linear features (LMLFs). The high resolution SAR data offers impressive detail on these infrastructures. In this work, we validate the time series results along a certain railway in China with high density leveling campaign. The Leveling points are distributed along the railway line and each two leveling points are 60 m disperse and the temporal interval is nearly one month. The study area is located in the west of Tianjin downtown, covering an area of 1.5 km \* 7.46 km. The validation results show that the average subsidence rate and time series of PS results are agreed well with that of these leveling points.

**Index Terms**—Railway, validation, subsidence, INSAR, high density leveling campaign

## 1. INTRODUCTION

In China, ground subsidence becomes one of the most severe and widespread geological hazard. Moreover, with the rapid development of urban cities, numerous large-scale man-made linear features (LMLFs), such as railways, highways, and power lines, have been constructed and they become economic lifeline of each region. The subsidence along these LMLFs has caused a lot of attention [1, 2], for not only the loss of financial investment but also lives at many places.

The station observation of deformation depending on leveling and GPS network, is costly, time consuming and laborious. By contrast, multi-temporal INSAR (MT-INSAR) analysis techniques were proved to be a powerful tool for deformation monitoring with high spatial-temporal resolution [3]. New generation SAR satellite can provide high resolution data of 1 m with short revisit of 11 days, which provides potential ability for identifying targets that need detailed information.

With applying optional MT-INSAR methods [4-7], high density of Permanent Scatters (PS) points can be detected and more precise subsidence monitoring information can be extracted with very high resolution SAR data. Subway tunnels and several highways in Shanghai urban area were monitored with time series INSAR data collected by Cosmo-skyMed satellites. The high resolution data of 3 m reveals impressive details of the ground surface deformation [8]. TomoSAR [9, 10] and higher-order permanent scatterers analysis [11, 12] were found to be useful ways to interpret the height and the deformation of building areas, especially for the very high buildings areas. Meanwhile, X-band PSI analysis makes possible the analysis and interpretation of the thermal expansion signal of single objects like buildings and bridges [13, 14]. Moreover, an extended PSI model is exploited to generate a new PSI product: thermal map [15]. Multiview TomoSAR points clouds were used to reconstruct building facades [16].

However, it is difficult to validate the time series results along LMLFs with high density leveling campaign. In this paper, we introduce the research carried out on the validation of time series analysis. We estimate the real precision of subsidence monitoring from high resolution MT-INSAR analysis by validating with leveling data of high spatial/temporal sampling. TSX MT-INSAR analysis for subsidence monitoring was carried out by using SARPROZ [17]. The output of the work will be useful to provide reference and will be helpful to further planning of subsidence monitoring over LMLFs.

## 2. STUDY AREA AND LEVELING DATA

The study area is located in the west of Tianjin downtown, covering an area of 1.5 km \* 7.46 km. The corresponding reflectivity map is extracted from high resolution TSX data and illustrated in Figure 1. The railway line is highlighted

with blue frame. The corresponding TSX PS results of study area can be extracted as illustrated in Figure 2. The color bar represents the subsidence rate ranges from -90 to -10 mm/yr.

Table 1 leveling data acquisitions

No.	acquisition time	No.	acquisition time	No.	acquisition time
1	200908	7	201003	13	201009
2	200910	8	201004	14	201010
3	200911	9	201005	15	201011
4	200912	10	201006	16	201012
5	201001	11	201007	17	201101
6	201002	12	201008		

42 leveling points are collected along the railway line and these leveling points are located as shown in figure 2. Table 1 gives the acquisition date of leveling data with the frequency of once every month and there are 17 times in total. The accuracy of leveling measurements is 2 mm/km according to Chinese secondary leveling measurement. As the exact acquisition date is unknown, 15th of each month is assumed. Moreover, the initial subsidence is assumed to be zero and starts from 15<sup>th</sup> August 2009. Leveling points are distributed along the railway line every 60 m. We discard the leveling points whose minimum distance from PS points is larger than 50 m. There are 41 leveling points left, numbered from ID 1 to 41.

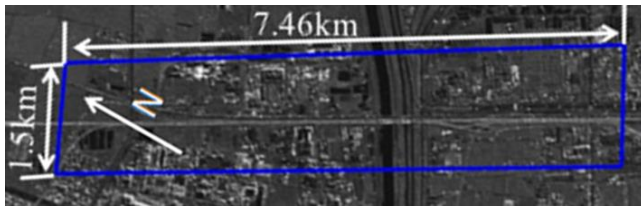


Figure 1 Study area. The blue frame marked the experimental area within 1.5 km \* 7.46 km.

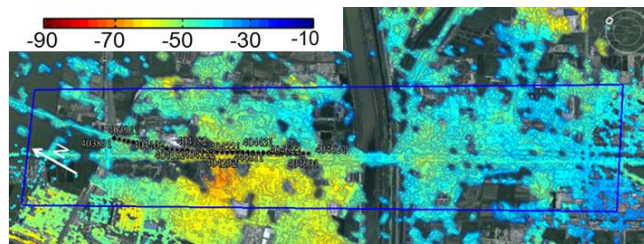


Figure 2 The linear subsidence velocity map along LOS direction. The colorbar represents the subsidence rate ranges from -90 to -10 mm/yr. The location of leveling points marked with black points.

### 3. THE VALIDATION PLAN

Our validation plan is divided into the following aspects in view of the characteristics of two distinct measurements of leveling and PS results.

(1) The average subsidence rate of PS results is extracted to compare with that of leveling data. Nearest neighbor method is adopted to select PS points.

(2) The time series of PS results are extracted to compare with leveling data. Because of the different acquisition time between leveling and TSX data, PS results are interpolated according to the acquisition time of leveling data.

(3) The average subsidence rates of all points from leveling and PS results are plot along the railway in order to evaluate the accuracy for describing subsidence of the railway line.

## 4. VALIDATION WITH LEVELING DATA

### 4.1 The average subsidence rate comparison

The average subsidence rate of nearest PS points was selected to compare with the leveling data. The comparison of average subsidence rate between PS results and leveling is summarized as shown in Table 2. During the comparison of average subsidence rate between PS results and leveling, the whole RMSE is 3.78 mm/yr, maximum error is 9.54 mm/yr and minimum is 0.06 mm/yr. The points with error larger than two times RMSE can be regarded as outliers and discarded. After coarse errors discarded, the whole RMSE is 2.55 mm/yr, maximum error is 4.74 mm/yr and minimum is 0.06 mm/yr. CC from linear regression is 0.82, very close to 1 (ideal condition). Then, the average subsidence rate comparison results show relatively good agreement between PS results and leveling measurements.

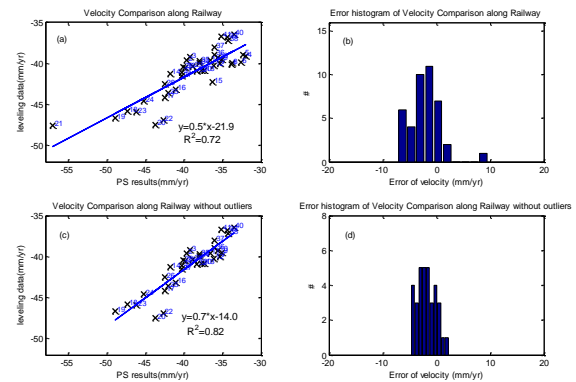


Figure 3 The regression analysis and error histogram of average subsidence velocity between PS results and leveling measurements along railway. (a) Regression of average velocity by using nearest neighbor method. (b) Error histogram of average velocity by using nearest neighbor method. (c) Regression of average velocity by using nearest neighbor method without outliers. (d) Error histogram of average velocity by using nearest neighbor method without outliers.

Meanwhile, the linear regression can be done between PS results and leveling. As shown in Figure 3(a), the CC between these two distinct measurements is 0.72, close to 1. The error histogram as illustrated in Figure 3(b) represents error ranging from -8 to 10 mm/yr. It is noted that the whole subsidence rate of this area is large, ranging from -70 to -50 mm/yr. After discarding outliers, the CC is 0.82, very close to 1. The error histogram represents error ranging -5 to 3 mm/yr.

Table 2 The comparison summary of average subsidence rate between PS results and leveling (unit: mm/yr)

Nearest neighbor	RMSE	MAX	MIN	CC	points
With outliers	3.78	9.54	0.06	0.72	40
Without outliers	2.55	4.74	0.06	0.82	34

The average subsidence velocity along the railway is plot according to point ID as Figure 4 shows. It is clearly see that InSAR results and leveling measurements keep high consistency. Both of them show spatial uneven subsidence in some regions. The average subsidence velocities increase at ID 17, ID 18, ID 19, ID 20, ID 23, ID 24 and ID 25 from both PS results and leveling, which demonstrates these two measurements are in good agreement with each other.

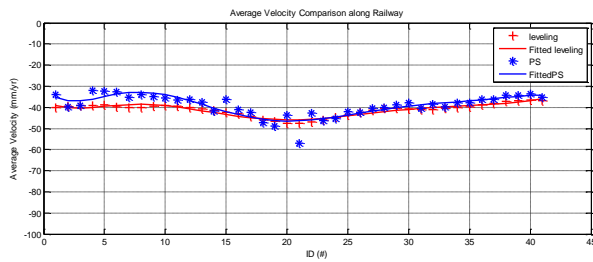


Figure 4 The average subsidence velocity comparison along the railway line.

## 4.2 The displacement comparison

In order to evaluate the accuracy of INSAR results, the displacement of PS results are extracted and compare with leveling at each point. Due to the different acquisition time between leveling and TSX data, PS results are interpolated according to the acquisition time of leveling data. Select the nearest PS point around each leveling point, extract the displacement along time series and interpolate the value according to the acquisition time of leveling data.

Table 3 The displacement comparison between PS results and leveling (unit: mm)

Nearest neighbor	RMSE	MAX	MIN	CC	points
With outliers	3.82	15.91	0.01	0.92	520
Without outliers	2.20	4.34	0.01	0.98	464

From Table 3, the accumulated RMSE is 3.82 mm, maximum error is 15.91 and minimum is 0.01 mm. After the coarser errors are discarded, the RMSE of 464 observations is 2.20 mm, maximum error is 4.34 and minimum is 0.01 mm.

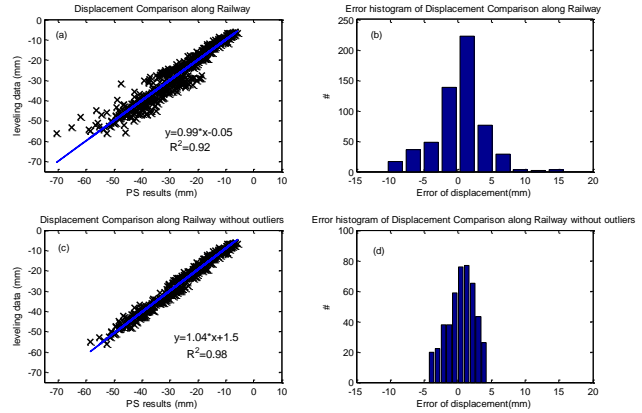


Figure 5 The regression analysis and error histogram of displacement between PS results and leveling measurements along railway. (a) Regression of displacement by using nearest neighbor method. (b) Error histogram of displacement by using nearest neighbor method. (c) Regression of displacement by using nearest neighbor method without outliers. (d) Error histogram of displacement by using nearest neighbor method without outliers.

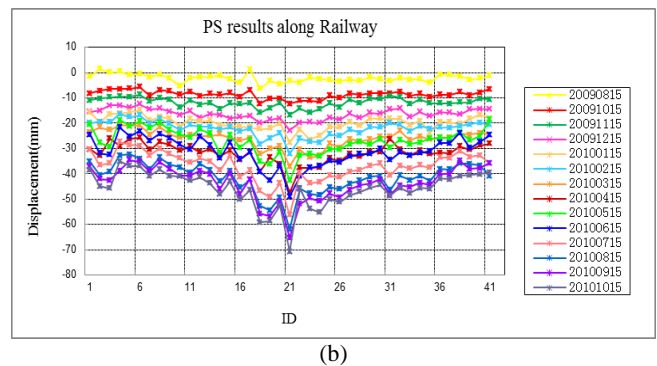
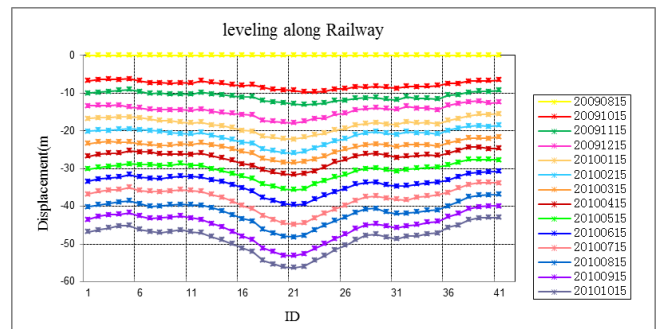


Figure 6 The displacements of PS results and leveling along the railway line. (a) The displacement of leveling. (b) The displacement of PS results.

The linear regression of displacement can be done between PS results and leveling. As shown in Figure 5(a), the CC between these two distinct measurements is 0.94, very close to 1. The error histogram as illustrated in Figure 5(b) represents error ranging from -10 to 15 mm. After discarding coarse error, the CC is 0.98, very close to 1. The error histogram represents error ranging -5 to 5 mm.

From the displacement comparison between PS results and leveling, we found that the displacements of most points detected by these two measurements are in good agreement. As Table 3 shows, the accumulated RMSE is 3.82 mm, and 2.20 mm after. CC from linear regression is 0.94 and 0.98 after discarding outliers, very close to 1 (ideal condition). The error ranges from -5 to 5 mm as Figure 5 (d). These results demonstrate the accuracy of displacement from PS results can achieve 2.20 mm compared with leveling measurement, which proves these two measurements show high consistency. That can be confirmed from Figure 6.

## 5. CONCLUSIONS

High resolution SAR data show high potential ability for monitoring LMLFs including highways, railways and power lines. Nevertheless, little validation has been carried out along these LMLFs, usually due to lack of the subsidence information of leveling points. The validation experiment shows the average velocity and displacement of PS results along the railway are well agreeing with that of leveling data, which provides reference and guidance for applying PS technique with high resolution SAR data to monitor subsidence of large-scale linear man-made infrastructures.

## 6. ACKNOWLEDGMENT

TerraSAR-X data are provided by Infoterra, Germany. The software we used for MT-INSAR analysis in this work is SARProz, developed by Daniele Perissin. The authors are very thankful to the partially support of the National Natural Science Foundation of China (grant No. 41431179), the Key Laboratory of Mapping from Space, National Administration of Surveying, Mapping and Geoinformation (No. K201408) and Guangxi Key Laboratory of Spatial Information and Geomatics (No. 13-051-14-16).

## 7. REFERENCES

[1] G. X. Liu, H. G. Jia, R. Zhang, H. X. Zhang, H. L. Jia, B. Yu, *et al.*, "Exploration of Subsidence Estimation by Persistent Scatterer InSAR on Time Series of High Resolution TerraSAR-X Images," *IEEE Journal of Selected Topics in Applied Earth Observations and Remote Sensing*, vol. 4, pp. 159-170, Mar 2011.  
 [2] Q. Luo, D. Perissin, Q. Li, H. Lin, and R. Duering, "Tianjin INSAR time series analysis with L- and X-band," in *Geoscience and Remote Sensing Symposium (IGARSS), 2011 IEEE International*, 2011, pp. 1477-1480.

[3] A. Ferretti, G. Savio, R. Barzaghi, A. Borghi, S. Musazzi, F. Novali, *et al.*, "Submillimeter accuracy of InSAR time series: Experimental validation," *IEEE Transactions on Geoscience and Remote Sensing*, vol. 45, pp. 1142-1153, May 2007.  
 [4] A. Ferretti, A. Fumagalli, F. Novali, C. Prati, F. Rocca, and A. Rucci, "A New Algorithm for Processing Interferometric Data-Stacks: SqueeSAR," *IEEE Transactions on Geoscience and Remote Sensing*, 2011.  
 [5] A. Ferretti, C. Prati, and F. Rocca, "Permanent scatterers in SAR interferometry," *IEEE Transactions on Geoscience and Remote Sensing*, vol. 39, pp. 8-20, Jan 2001.  
 [6] D. Perissin, A. Ferretti, R. Piantanida, D. Piccagli, C. Prati, F. Rocca, *et al.*, "Repeat-pass SAR interferometry with partially coherent targets," 2007, pp. 26-30.  
 [7] A. Hooper, H. Zebker, P. Segall, and B. Kampes, "A new method for measuring deformation on volcanoes and other natural terrains using InSAR persistent scatterers," *Geophysical Research Letters*, vol. 31, Dec 2004.  
 [8] D. Perissin, W. Zhiying, and L. Hui, "Shanghai subway tunnels and highways monitoring through Cosmo-SkyMed Persistent Scatterers," *ISPRS Journal of Photogrammetry and Remote Sensing*, vol. 73, pp. 58-67, 2012.  
 [9] G. Fornaro, D. Reale, and F. Serafino, "Four-dimensional SAR imaging for height estimation and monitoring of single and double scatterers," *IEEE Transactions on Geoscience and Remote Sensing*, vol. 47, pp. 224-237, 2009.  
 [10] G. Fornaro, F. Serafino, and D. Reale, "4-D SAR Imaging: The Case Study of Rome," *IEEE Geoscience and Remote Sensing Letters*, vol. 7, pp. 236-240, 2010.  
 [11] A. Ferretti, M. Bianchi, C. Prati, and F. Rocca, "Higher-order permanent scatterers analysis," *Eurasip Journal on Applied Signal Processing*, vol. 2005, pp. 3231-3242, 2005.  
 [12] T. Balz, W. Lianhuan, M. Jendryke, D. Perissin, and L. Mingsheng, "TomoSAR and PS-InSAR analysis of high-rise buildings in Berlin," in *IGARSS 2012 - 2012 IEEE International Geoscience and Remote Sensing Symposium, 22-27 July 2012*, Piscataway, NJ, USA, 2012, pp. 447-50.  
 [13] O. Monserrat, M. Crosetto, M. Cuevas, and B. Crippa, "The Thermal Expansion Component of Persistent Scatterer Interferometry Observations," *IEEE Geoscience and Remote Sensing Letters*, vol. 8, pp. 864-8, 2011.  
 [14] G. Fornaro, D. Reale, and S. Verde, "Bridge thermal dilation monitoring with millimeter sensitivity via multidimensional SAR imaging," *IEEE Geoscience and Remote Sensing Letters*, vol. 10, pp. 677-81, 07/ 2013.  
 [15] M. Crosetto, O. Monserrat, M. Cuevas-Gonzalez, N. Devanthery, G. Luzi, and B. Crippa, "Measuring thermal expansion using X-band persistent scatterer interferometry," *ISPRS Journal of Photogrammetry and Remote Sensing*, vol. 100, pp. 84-91, 02/ 2015.  
 [16] X. X. Zhu and M. Shahzad, "Facade Reconstruction Using Multiview Spaceborne TomoSAR Point Clouds," *IEEE Transactions on Geoscience and Remote Sensing*, vol. 52, pp. 3541-3552, Jun 2014.  
 [17] D. Perissin, "SARPROZ software manual," <http://www.sarproz.com/software-manual/>.